Effect of geometry and interfacial resistance on current distribution and energy dissipation at metal/superconductor junctions

Meilin Liu and Lutgard C. De Jonghe
Department of Materials Science and Mineral Engineering, University of California, and Center for Advanced Materials, Materials and Chemical Sciences Division, Lawrence Berkeley Laboratory, 1 Cyclotron Road, Berkeley, California 94720

(Received 5 July 1988; accepted 14 December 1988)

Potential and current distributions and local energy dissipation due to Joule heating in metal-superconductor junctions have been computed as a function of geometric parameters and interfacial resistance. The primary current distribution and power dissipation are highly nonuniform in the system. The secondary current distribution and power dissipation, however, become more uniform as the interfacial resistance increases. Analysis indicates that zero contact resistance is not a stable situation since the primary distribution leads to local current densities exceeding the critical current density of the superconducting phase near the corner of the junction. Local contact failure might then initiate. A finite contact resistance is necessary for a practical application, and the minimum value of the contact resistance can be estimated from the operating current density (j_{avg}) of the device and the critical current density (j_{cri}) of the superconducting phase. To obtain an optimum value of the contact resistance, however, one further has to take into consideration the stability and reliability of the device performance, which is, in turn, directly related to the uniformity of the current distribution and power dissipation, to temperature fluctuation of the superconducting phases brought about by local power dissipation, and to the thermal management of the system. Furthermore, a nonuniform contact resistance layer of appropriate profile can redistribute the current more effectively and more uniformly and hence reduce the total power dissipation in the system for a given j_{max}/j_{avg} ratio obtained by a uniform resistance layer.

I. INTRODUCTION

The use of superconducting materials in devices most often requires the incorporation of metal/superconductor junctions. Examples of two commonly encountered geometries of such junctions are sketched in Figs. 1(a) and 1(b). Figure 1(a) corresponds to one in which a thin or thick film of the superconductor, deposited on an insulating substrate, is contacted by a metal lead. The geometry of Fig. 1(b) would be encountered when a fracture has occurred in a metal-cladded superconducting wire. In both of these examples, the current densities at the metal-superconductor junctions, the m/s junctions, can be expected to be highly nonuniform and peak sharply at the corners of the m/s junction, as indicated schematically in Fig. 1.

As is well known in electrochemical applications involving current distributions at electrodes, one must distinguish between a primary current distribution which assumes no interface overpotential, and a more realistic one, the secondary current distribution, which takes into account the possibility of a finite interface overpotential. The problem of finding the current distribution at an m/s junction is in many aspects quite similar to the electrochemical problem of current distributions on electrodes and should, in addition, take into account the local energy or Joule heat generation at the junction. A primary current distribution will, in fact, exhibit a singularity at the corner of the m/s

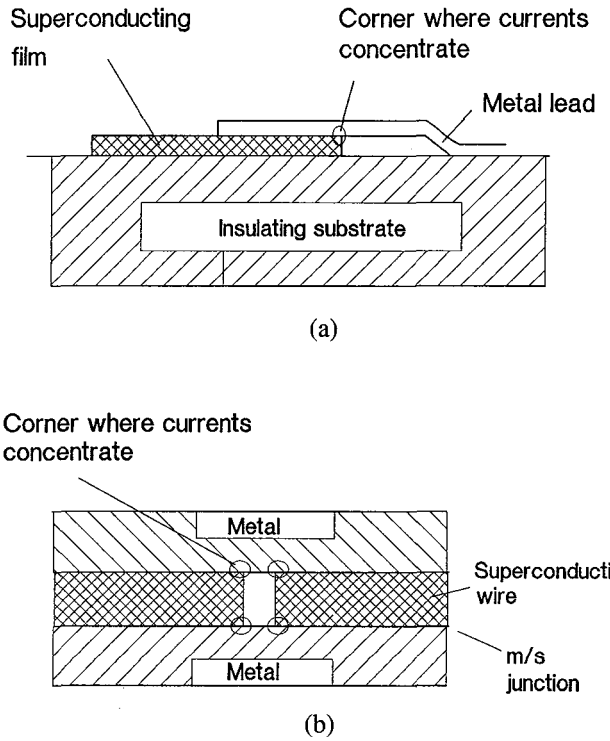

FIG. 1. Geometry of superconductor devices: (a) superconductor film deposited on an insulating substrate and contacted by a metal lead; (b) metal-cladded superconducting wire with a fracture.

junction which could in principle lead to large local energy losses in the adjacent metal, and even to contact failure initiation.

To analyze the problem of current distribution and energy loss, the electrode problem in an equivalent electrochemical cell of appropriate geometry is considered. The current distribution in rectangular electrochemical cells with similar configuration, as shown in Fig. 2(b), has been treated in the literature.[1–3] The primary current distribution predicts infinite current densities at the marked corner of the electrode. This singularity in an electrochemical system is, however, removed by various processes that lead to interface overpotentials and current redistribution: the finite kinetics of electrochemical reactions, the transport rate limitation of electrochemical species, or the changes in the electrode configuration brought about by electrodeposition or dissolution.[4–6] In the m/s junction system, these processes modifying the primary current distribution are not present. At the same time, the average current densities are many orders of magnitude higher than in electrochemical systems, making local current concentration and local energy loss consideration due to Joule heating much more important. However, a practical parameter that allows for a controlled modification of the current distribution is available: the m/s interface resistance. In this paper, the effects of the m/s junction geometry and interface resistance on the current distribution and on the energy dissipation are discussed. A rectangular domain with an interrupted junction, as shown in Fig. 2(b), corresponding to the situations sketched in Fig. 1, has been chosen for the analysis.

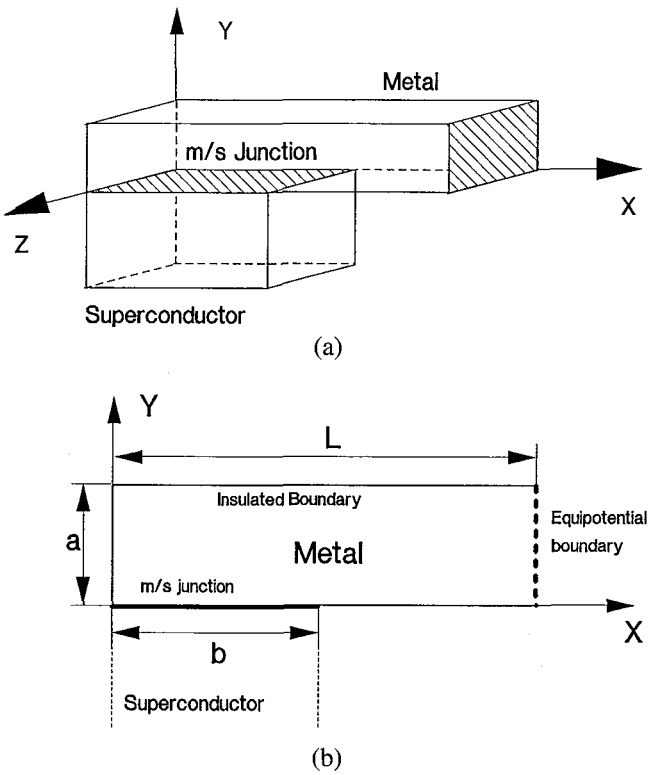

FIG. 2. (a) Geometry of metal-superconductor junction; (b) simplified 2-dimensional model for calculation.

II. MATHEMATICAL MODEL

Consider a superconductor/metal junction as pictured in Fig. 2(a). If the potential or current distribution is independent of z, the system is reduced to a two-dimensional problem, as shown in Fig. 2(b). Under the assumption that the bulk metal phase is isotropic and the metal superconductor contact interface is uniform, with the superconductor at equipotential, the potential, $\Phi(x, y)$, must satisfy Laplace's equation:

$$\partial^2\Phi/\partial x^2 + \partial^2\Phi/\partial y^2 = 0 \quad (1)$$

within the domain of the metal phase (Ω_m). The following boundary conditions apply:

(1) The derivatives of the potential Φ normal to the insulated boundary, Γ_1, vanish at the boundary, i.e.

$$\nabla\Phi \cdot \mathbf{n} = 0 \quad \text{on } \Gamma_1 \quad (2)$$

(2) The potential at the end of the metal phase is constant for the ratio of L/b sufficiently large:

$$\Phi(L, y) = \Phi_0 \quad \text{on } \Gamma_2 \quad (3)$$

(3) The potential at the metal side of the m/s junction is specified as

$$\Phi(x, 0) = \Phi_1 - \Delta V_i(x) \quad \text{on } \Gamma_3 \quad (4)$$

where Φ_1 is the potential of the superconducting phase and ΔV_i is the potential drop across the interface which depends on the nature of the m/s contact and the current density at the interface. Therefore, the surface of the metal phase adjacent to the m/s junction is not an equipotential surface if the contact resistance is finite. For a linear contact, ΔV_i can be approximated, at sufficient normal current densities, by

$$\Delta V_i(x) = V_0 + \alpha \cdot j_n(x) \quad (5)$$

where V_0 is a constant, α is the specific interfacial resistance (ohm-cm^2), and j_n is the current density normal to the contact interface. This type of contact resistance has been reported recently for several metal-superconductor junctions, including aluminum-YBCO, noble metal (silver, gold)-YBCO, and indium-YBCO junctions.[7–9]

III. NUMERICAL CALCULATION

In a finite element method, the potential within the metal domain can be approximated by an expression of the form

$$\sum_{j=1}^{N} \phi_j \Psi_j(\xi, \eta) \quad (6)$$

where the ϕ_j are the nodal potential values to be determined, N is the number of nodes in an element, and the $\Psi_j(\xi, \eta)$ are the approximation functions (in natural coordinates ξ and η) associated with each node. By substituting the above approximation into Eq. (1) and minimizing the weighted residual using $\Psi_j(\xi, \eta)$ as a weighing function,

the boundary-value problem, defined in Eqs. (1)–(4), can be transferred to the following matrix equation for each element:

$$[\mathbf{K}^{(e)}] \cdot \{\phi^{(e)}\} = \{\mathbf{F}^{(e)}\} \tag{7}$$

where

$$K_{ij}^{(e)} = \int_{\Omega_e} [(\partial\Psi_i/\partial x)(\partial\Psi_j/\partial x) + (\partial\Psi_i/\partial y)(\partial\Psi_j/\partial y)]\, d\Omega_e \tag{8}$$

$$F_i^{(e)} = \oint_{\Gamma_e} \Psi_i[(\partial\Phi/\partial x) + (\partial\Phi/\partial y)]\, ds \tag{9}$$

with Ω_e and Γ_e representing the domain and the boundary of the element, respectively. Rectangular elements with 9 nodes and piecewise quadratic interpolation functions are used in the calculation.

The assembly of element equations gives the following global matrix equation:

$$[\mathbf{K}] \cdot \{\mathbf{U}\} = \{\mathbf{F}\} \tag{10}$$

The fact that the potential of the superconductor phase (Φ_1) and the potential at Γ_2 (Φ_0) are known and the remaining potentials ($\mathbf{U}_2$) and the potential gradients at Γ_2 and Γ_3 ($\mathbf{f}_0$ and $\mathbf{f}_n$) are unknown provides us the motivation to rearrange and partition the matrix equation as follows:

$$\begin{pmatrix} [\mathbf{K}_{11}] & [\mathbf{K}_{12}] & [\mathbf{K}_{13}] \\ [\mathbf{K}_{21}] & [\mathbf{K}_{22}] & [\mathbf{K}_{23}] \\ [\mathbf{K}_{31}] & [\mathbf{K}_{32}] & [\mathbf{K}_{33}] \end{pmatrix} \times \begin{pmatrix} \{\Phi_1 - V_0\} - \alpha\sigma\{\mathbf{f}_n\} \\ \{\mathbf{U}_2\} \\ \{\Phi_0\} \end{pmatrix} = \begin{pmatrix} [\mathbf{P}_n]\{\mathbf{f}_n\} \\ \{\mathbf{0}\} \\ [\mathbf{p}_0]\{\mathbf{f}_0\} \end{pmatrix} \tag{11}$$

where V_0 and α are as defined in Eq. (5) and σ is the conductivity of the metal phase. The potential gradients at the boundaries, $\{\mathbf{f}_n\}$ and $\{\mathbf{f}_0\}$, are given by

$$\{\mathbf{f}_n\} = (\partial\{\Phi\}/\partial y)_{y=0}, \qquad 0 \le x \le b \tag{12a}$$

$$\{\mathbf{f}_0\} = (\partial\{\Phi\}/\partial x)_{x=L}, \qquad 0 \le y \le a \tag{12b}$$

and the diagonal matrix $[\mathbf{P}_n]$ contains the elements of boundary integration of the interpolation function along the m/s junction and $[\mathbf{P}_0]$ contains the elements of boundary integration along the end of metal phase (Γ_2).

To calculate directly the potential gradient distribution at the m/s junction with a uniform resistive layer, the matrix Eq. (11) can be rewritten as

$$\begin{pmatrix} -\alpha\sigma[\mathbf{K}_{11}] - [\mathbf{P}_n] & [\mathbf{K}_{12}] & [\mathbf{0}] \\ -\alpha\sigma[\mathbf{K}_{21}] & [\mathbf{K}_{22}] & [\mathbf{0}] \\ -\alpha\sigma[\mathbf{K}_{31}] & [\mathbf{K}_{32}] & -[\mathbf{P}_0] \end{pmatrix} \begin{pmatrix} \{\mathbf{f}_n\} \\ \{\mathbf{U}_2\} \\ \{\mathbf{f}_0\} \end{pmatrix} = -\begin{pmatrix} [\mathbf{K}_{11}] \\ [\mathbf{K}_{21}] \\ [\mathbf{K}_{31}] \end{pmatrix} \{\Phi_1 - V_0\} - \begin{pmatrix} [\mathbf{K}_{13}] \\ [\mathbf{K}_{23}] \\ [\mathbf{K}_{33}] \end{pmatrix} \{\Phi_0\} \tag{13}$$

Obviously, this equation can further be reduced to

$$\begin{pmatrix} -\alpha\sigma[\mathbf{K}_{11}] - [\mathbf{P}_n] & [\mathbf{K}_{12}] \\ -\alpha\sigma[\mathbf{K}_{21}] & [\mathbf{K}_{22}] \end{pmatrix} \times \begin{pmatrix} \{\mathbf{f}_n\} \\ \{\mathbf{U}_2\} \end{pmatrix} = -\begin{pmatrix} [\mathbf{K}_{11}] \\ [\mathbf{K}_{21}] \end{pmatrix} \{\Phi_1 - V_0\} - \begin{pmatrix} [\mathbf{K}_{13}] \\ [\mathbf{K}_{23}] \end{pmatrix} \{\Phi_0\} \tag{14}$$

Meanwhile, instead of solving for the current distribution for a uniform contact resistance layer, the optimum distribution of a nonuniform interfacial resistance ($\{\alpha\}$) for a required current distribution ($\{\mathbf{f}_n\}$), can alternatively be calculated from the following equivalent equation:

$$\begin{pmatrix} -[\mathbf{K}_{11}][\mathbf{f}_n] & [\mathbf{K}_{12}] \\ -[\mathbf{K}_{21}][\mathbf{f}_n] & [\mathbf{K}_{22}] \end{pmatrix} \begin{pmatrix} \sigma\{\alpha\} \\ \{\mathbf{U}_2\} \end{pmatrix} = -\begin{pmatrix} [\mathbf{K}_{11}] \\ [\mathbf{K}_{21}] \end{pmatrix} \{\Phi_1 - V_0\} - \begin{pmatrix} [\mathbf{K}_{13}] \\ [\mathbf{K}_{23}] \end{pmatrix} \{\Phi_0\} + \begin{pmatrix} [\mathbf{P}_n]\{\mathbf{f}_n\} \\ [\mathbf{0}] \end{pmatrix} \tag{15}$$

where $[\mathbf{f}_n]$ now is a diagonal matrix and $\{\alpha\}$ is a vector

$$[\mathbf{f}_n] = \begin{pmatrix} f_1 & & & \\ & f_2 & & \\ & & \ddots & \\ & & & f_m \end{pmatrix} \qquad \{\alpha\} = \begin{pmatrix} \alpha_1 \\ \alpha_2 \\ \vdots \\ \alpha_m \end{pmatrix} \tag{16}$$

These equations have been solved on a VAX-8650 (VMS) computer with NAG libraries.

IV. ENERGY DISSIPATION

As current flows through the system, two Joule heating processes contribute simultaneously to the energy loss. One is in the bulk metal phase and the other is at the m/s junction.

The Joule heat production rate (Watt) in the bulk metal phase is given by

$$dQ_b/dt = \int_{\Omega_m} \mathbf{j} \cdot \mathbf{j}/\sigma\, d\Omega_m \tag{17}$$

where $\mathbf{j}$ is the current density, and σ is the conductivity of the bulk metal phase in domain Ω_m. Obviously, the local power dissipation in the metal phase is proportional to $\mathbf{j} \cdot \mathbf{j}$.

Variational analysis indicates on the one hand that, subject to the constraint of a constant total current

$$J = \int_0^b j_n(x)\, dx = \text{constant} \tag{18}$$

dQ_b/dt first decreases rapidly as the current density normal to the junction becomes more uniform and reaches a lower

limit when the normal current density becomes completely uniform, i.e., when

$$j_n(x) = j_{avg} \qquad 0 \le x \le b \tag{19}$$

The average current density, j_{avg}, is defined as

$$j_{avg} = (1/b)\int_0^b j_n(x)\,dx \tag{20}$$

On the other hand, the Joule heat production rate (Watt) at the contact interface, expressed as

$$dQ_i/dt = \int_0^b \Delta V_i(x) \cdot j_n(x)\,dx \tag{21}$$

increases as the current distribution becomes more uniform as a consequence of increase of interfacial resistance. The local power dissipation at the m/s junction is proportional to j_n^2.

The total energy dissipation rate in the system is then the sum of the two heating processes which are approximated by the expressions

$$dQ_b/dt = \sigma\int_{\Omega_m} [(\partial U/\partial x)^2 + (\partial U/\partial y)^2]\,d\Omega_m \tag{22}$$

and

$$dQ_i/dt = J \cdot V_0 - \sigma\int_0^b [\Delta V_i(x) - V_0](\partial U/\partial y)_{y=0}\,dx \tag{23}$$

The total power dissipation can also be estimated from the effective total resistance of the system, R_{eff}, which is given by

$$R_{eff} = (\Phi_1 - \Phi_0)\Big/\int_0^b j_n(x)\,dx \tag{24}$$

V. RESULTS AND DISCUSSION

A. Primary distribution and junction geometry

When the contact resistance is zero, the potential at the metal side of the m/s junction is uniform and the current distribution is completely determined by junction geometry, with an infinite current density at the marked corner of the junction (i.e., $j_n \to \infty$ at $x = b$). The primary current distributions at the m/s interface for different junction geometries are shown in Fig. 3. Evidently, the current distribution becomes more uniform as the ratio of a/b increases provided that L is large enough so that $\Phi(L, y)$ at Γ_2 is constant. In other words, at constant b, the primary current distribution becomes more uniform as the dimension a increases, and at constant a, the current distribution becomes more uniform as dimension b decreases, if the influence of L is excluded. Obviously, the dimension L has no effect on current distribution as long as the potential at the end of the metal phase is uniform. The minimum dimension L below which $\Phi(L, y)$ becomes nonuniform depends on dimensions a and b. Figure 4 shows the effect of the geometric parameters on the primary potential distribution at the tail region of the metal phase. Clearly, the minimum length L at which $\Phi(L, y)$ is practically uniform increases as the ratio a/b increases. These geometric effects could provide guidance for device design.

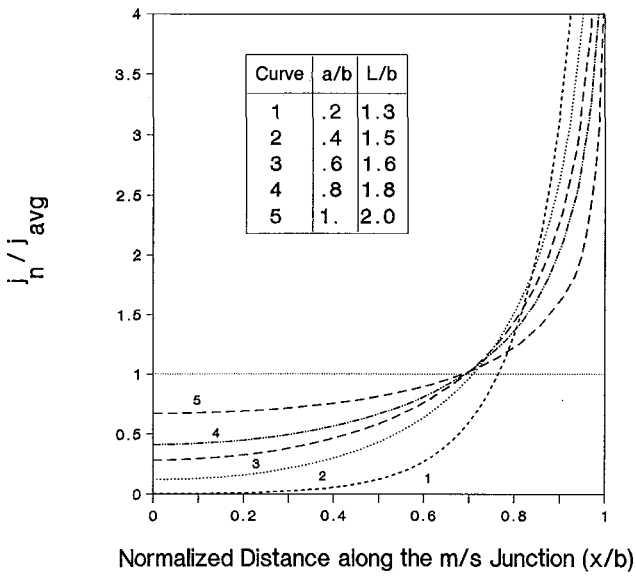

FIG. 3. Primary current distribution at metal-superconductor junctions of different geometry. The maximum value of the current density is infinite at the marked corner of the junction ($j_n/j_{avg} \to \infty$ at $x = b$).

B. Secondary distribution and interfacial resistance

When a finite contact resistance is taken into consideration, the nonuniform current distribution at the m/s junction results in nonuniform potential drop across the interface so that the surface of the metal phase adjacent to the m/s junction is no longer an equipotential surface [see Eqs. (4) and (5) and the current distribution in Fig. 3]. It is the modification of the potential at the boundary Γ_3 due to the presence of the contact resistance that redistributes the secondary currents more nearly uniform than the primary currents, as shown in Fig. 5. Unlike the primary distribution, the secondary current distribution depends not only on the geometry but also on the electrical properties of the bulk phase and the nature of the metal-superconductor interface.

The current density normal to the interface is plotted in Fig. 5 for different normalized interfacial resistance R, which is defined as

$$R = \alpha \cdot \sigma/b \tag{25}$$

where α is the interfacial resistance (ohm-cm^2), σ is the conductivity (ohm^{-1} cm^{-1}) of the bulk metal phase, b is the length (cm) of the junction as defined in Fig. 2(b), and hence R is dimensionless.

The computations (shown in Fig. 5) clearly indicate that as the dimensionless interfacial resistance (R) increases, the current distribution at the interface becomes

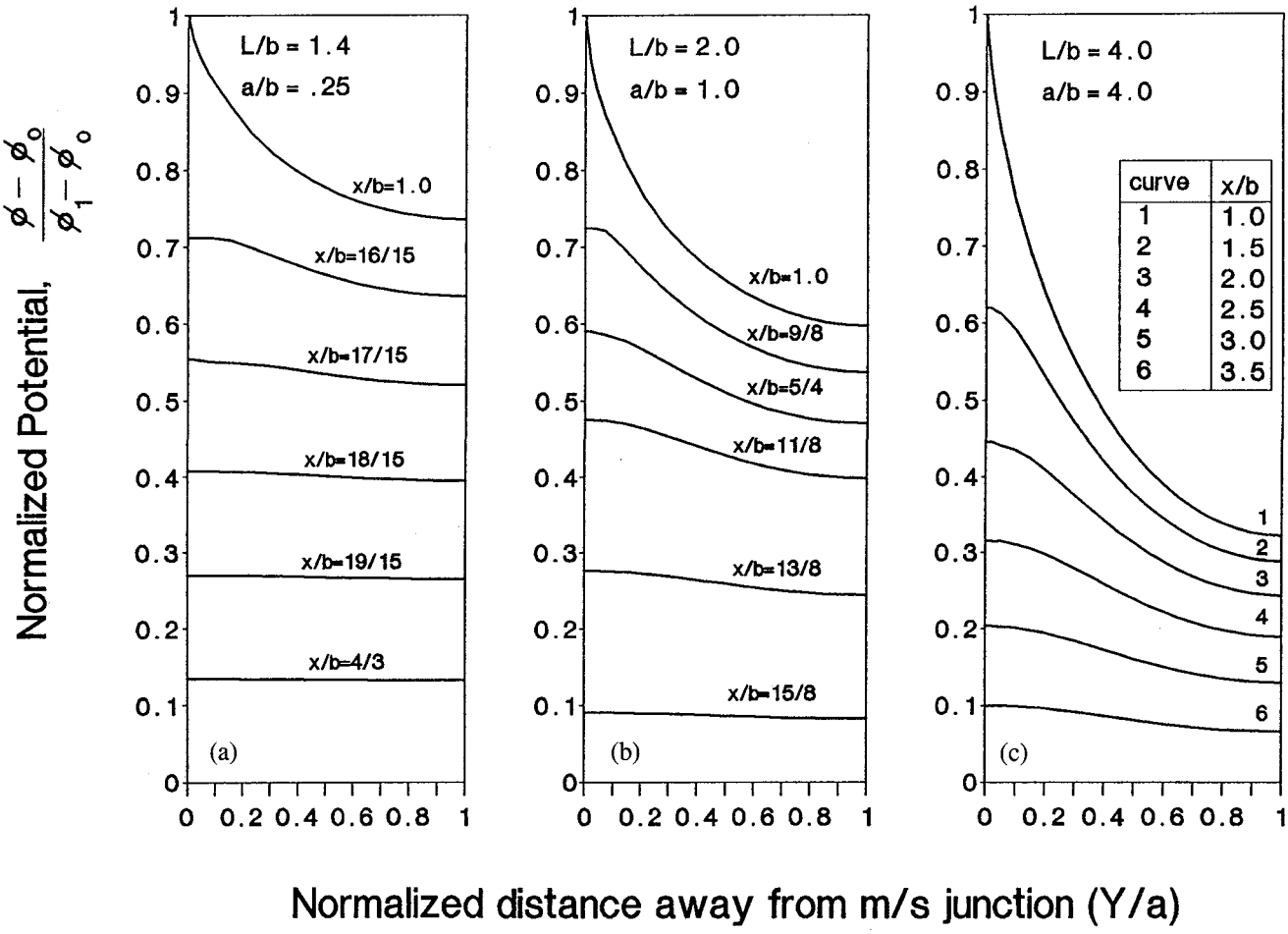

FIG. 4. Primary potential distribution at the tail region of the metal phase for (a) $a/b = 0.25$, $L/b = 1.4$; (b) $a/b = 1.0$, $L/b = 2.0$; and (c) $a/b = 4.0$, $L/b = 4.0$.

more uniform. In other words, the increase of the interfacial resistance, the increase of the conductivity of the bulk metal phase, or the decrease of the dimension b will make the secondary current distribution more uniform.

The effects of geometry on the secondary distributions are similar to those on the primary distribution, as is evident from the comparison of Fig. 5(a) and Fig. 5(b).

C. Critical current density and minimum contact resistance

It is obvious that zero contact resistance is unstable since the current singularity at the corner ($x = b$) of the junction leads to a local current density exceeding the critical current density of the superconducting phase. Local contact failure initiation might then result. Practically, a finite contact resistance is necessary to modify the current distribution. The minimum value of the contact resistance can be determined from the operating or average current density normal to the m/s junction and the critical current density of the superconducting phase. The criterion is that the contact resistance should be sufficiently large that the current density normal to the m/s junction at the corner ($x = b$) be less than or, at most, equal to the critical current density of the superconducting phase, i.e.

$$j_{max} \leq j_{cri} \tag{26}$$

The normalized maximum current densities at the corner of the m/s junction (j_{max}/j_{avg}) are plotted in Fig. 6 against the normalized interfacial resistance (R) for various geometries. The minimum contact resistance, R_{min}, for a given j_{avg} and j_{cri} can be determined from this diagram.

If the device is operated at a current level much lower than the critical current density, the minimum contact resistance will be very small. To estimate the optimum value of the contact resistance, however, one in addition has to take into consideration the stability and reliability of the device performance, which is, in turn, directly related to the uniformity of current distribution and power dissipation, to temperature fluctuation of the superconducting phases brought about by local power dissipation, and to the thermal management of the system.

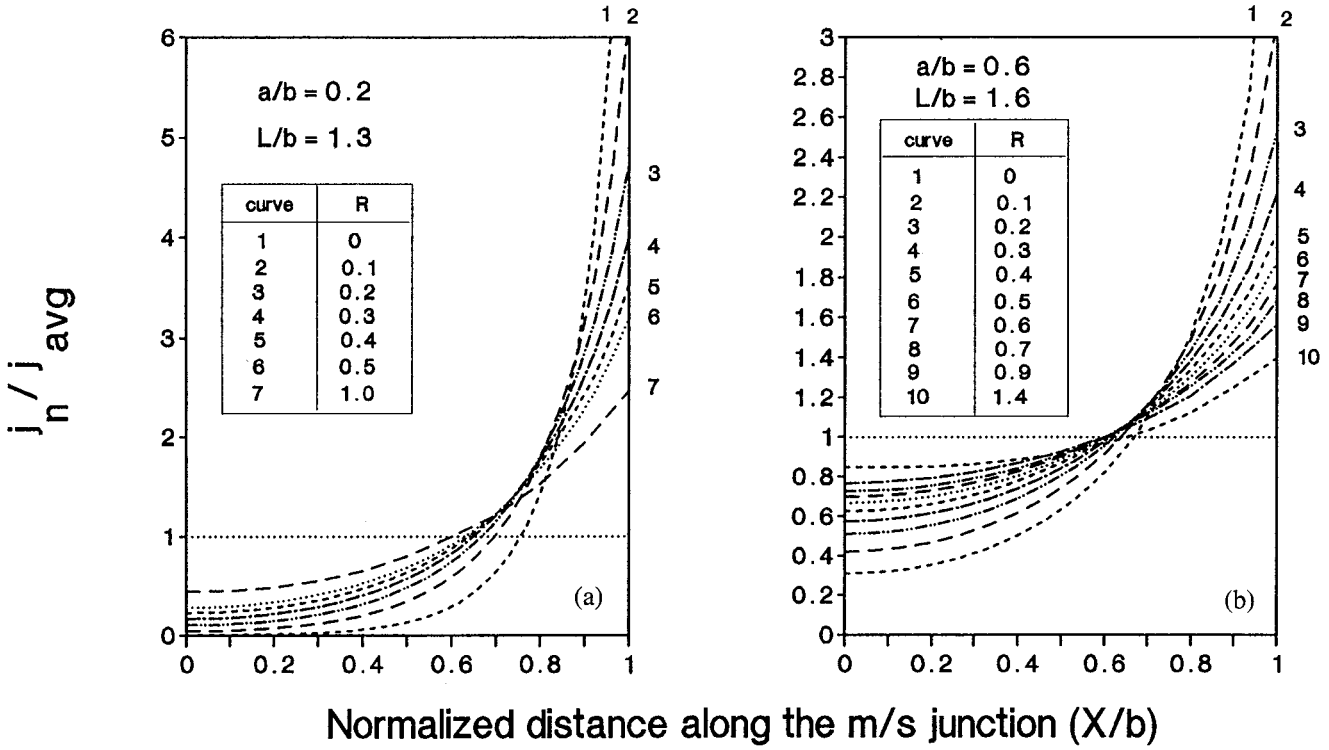

FIG. 5. Secondary current distribution at metal/superconductor junction for (a) $a/b = 0.20$, $L/b = 1.3$ and (b) $a/b = 0.6$, $L/b = 1.6$. Curve 1 represents the primary current distribution ($j_n/j_{avg} \rightarrow \infty$ at $x = b$). Curves 2–7 in (a) and curves 2–10 in (b) represent the secondary current distribution for different contact resistances.

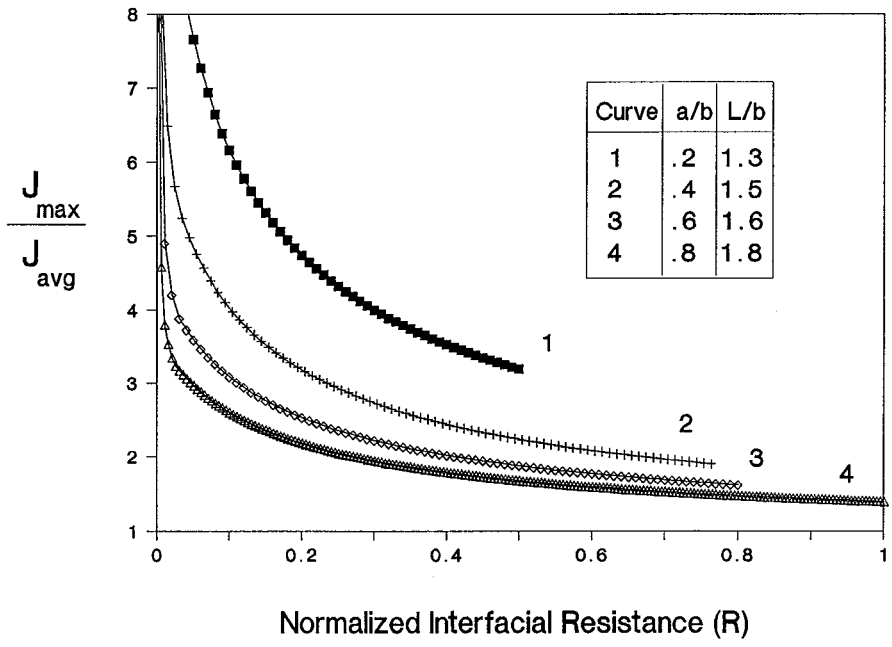

FIG. 6. Dependence of normalized maximum current densities on the normalized interfacial resistance.

D. Power dissipation and optimum interfacial resistance distribution

Since the local power dissipation is proportional to the square of the local current [see Eqs. (17) and (21)], the primary and secondary distribution of the Joule heat production rate near the m/s junction should be similar to the square of the currents shown in Fig. 3 and Fig. 5. When the contact resistance is very low, the power dissipation is highly concentrated near the corner of the m/s junction, which could lead to local overheating.

The power dissipation in the bulk metal phase, at the m/s junction, and the total power dissipation in the system are plotted in Fig. 7 as a function of the normalized interfacial resistance. As the interfacial resistance increases, the Joule heat production rate *decreases* in the bulk metal phase and increases at the interface. While the total power dissipation in the system slightly increases, its distribution along the m/s junction becomes more uniform.

The dependence of power dissipation on the uniformity of current distribution or the j_{max}/j_{avg} ratio is shown in Fig. 8 for the case where a uniform contact resistive layer is applied to the m/s junction. It is clear that the power dissipation increases dramatically as current distribution becomes more uniform as a result of an increased interface resistance. In other words, as the resistance of a uniform interface layer increases, further improvement in current uniformity becomes less useful.

Shown in Fig. 9 are the optimum distributions of the interfacial resistance for completely uniform current distribution at the m/s junctions with different geometries.

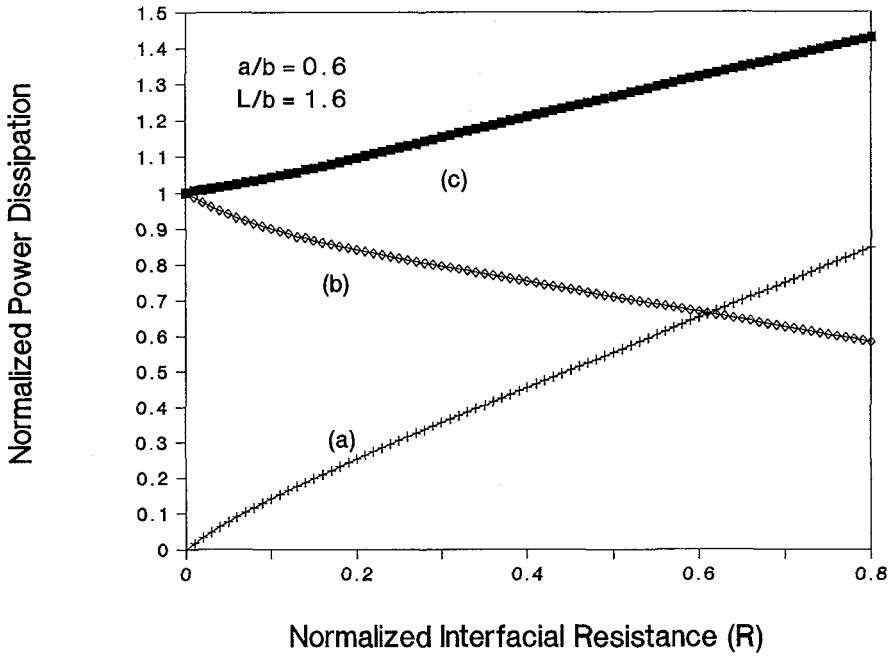

FIG. 7. Dependence of power dissipation on interfacial resistance for $a/b = 0.6$ and $L/b = 1.6$: (a) at the m/s junction, $(dQ_i/dt)/(dQ/dt)_{R=0}$; (b) in the bulk metal phase, $(dQ_b/dt)/(dQ/dt)_{R=0}$; and (c) the total power dissipation in the system, $(dQ/dt)/(dQ/dt)_{R=0}$.

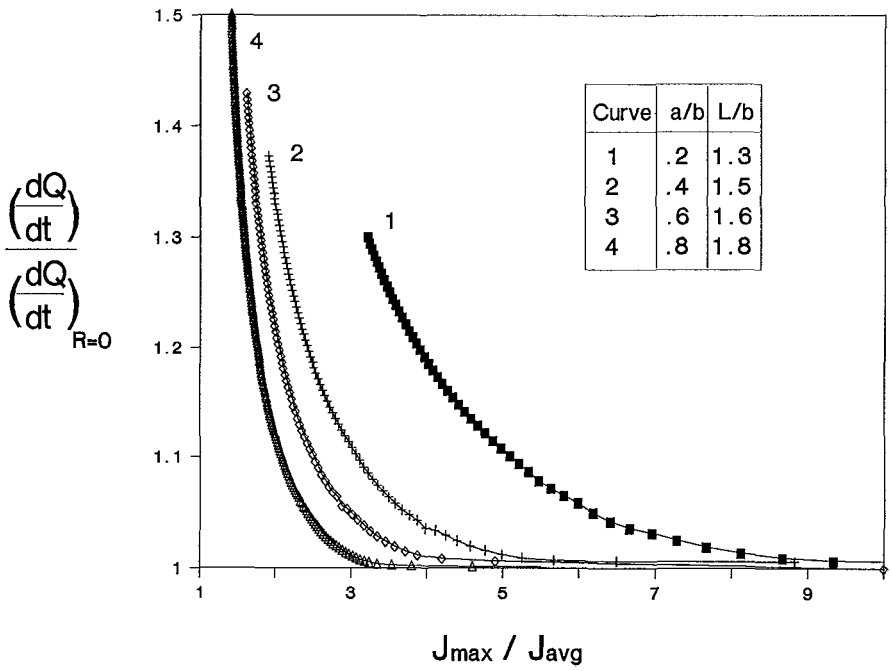

FIG. 8. Dependence of total power dissipation on uniformity of current distribution at the m/s junction with a uniform resistance of the contact layer.

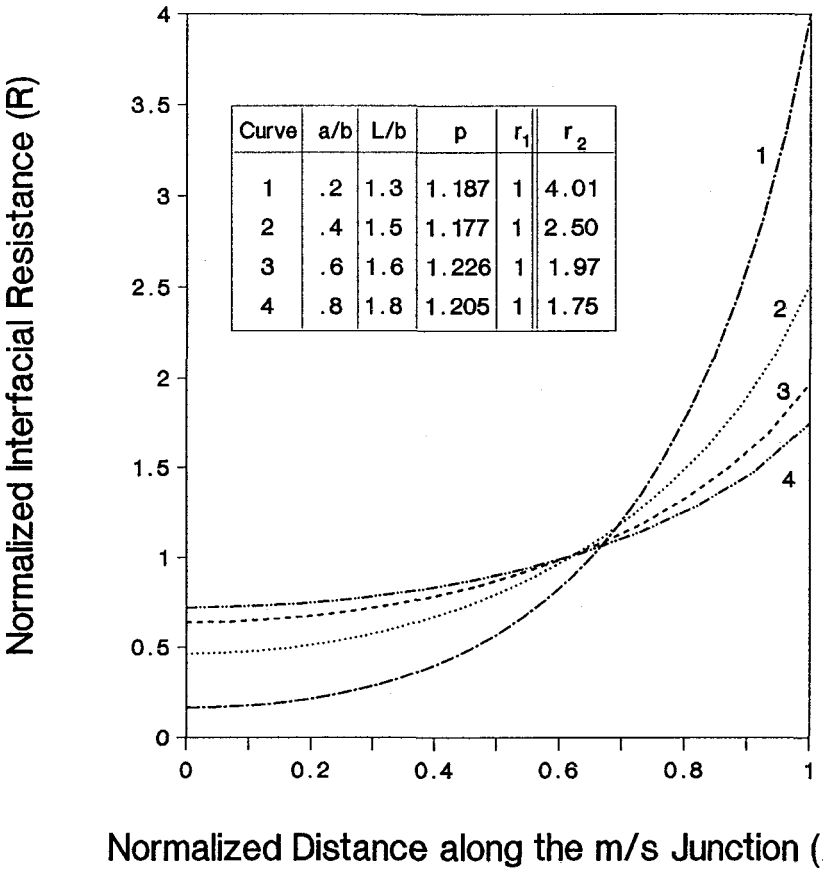

FIG. 9. Optimum distribution of interfacial resistance for uniform current distribution at the m/s junction. The corresponding total power dissipation, $P = (dQ/dt)/(dQ/dt)_{R=0}$, and the current ratios, $r_1 = j_{max}/j_{avg}$, are tabulated in the table. Listed in the last column of the table are the current ratios, $r_2 = j_{max}/j_{avg}$, determined from Fig. 8 at the corresponding power dissipation shown in column 4.

The corresponding normalized total power dissipation and j_{max}/j_{avg} ratios are tabulated in the table on the figure. The j_{max}/j_{avg} ratios for uniform resistance of the contact layer at the corresponding power dissipation are also listed in the last column of the table. It is clear that a nonuniform resistive layer, with an appropriate profile, can redistribute the current more effectively and more uniformly and hence reduce the total power dissipation for a given j_{max}/j_{avg} ratio obtained by a uniform resistance layer. This effect becomes more evident as the ratio of a/b decreases. The optimum distribution of the interfacial resistance for a required j_{max}/j_{avg} ratio can be calculated using Eq. (15) and can be precisely achieved through materials processing.

E. Inhomogeneity of superconductive materials

The high T_c ceramic superconductive materials are often inhomogeneous and contain some nonsuperconducting phases.

According to London theory and Meissner effect,[10,11] the current carried by a pure superconducting phase is confined to the thin surface layer of the material with penetration depth

$$\lambda_L = (m^*/\mu_0 e^{*2} n_s^*)^{1/2} \quad (27)$$

for particles of charge e^* and mass m^* in concentration n_s^*. The current density is exponentially damped from the external surface and virtually vanishes in the bulk of the material. Therefore, as long as the surface layer (with thickness of λ_L) of the inhomogeneous superconductive material near the m/s junction is in a superconducting state, the potential at the superconductor side of the m/s junction will be uniform and hence the current distribution and power dissipation at the m/s junction and in the metal phase will remain the same as discussed above, no matter how the nonsuperconducting phases are distributed inside the inhomogeneous superconductive materials.

If nonsuperconducting phases are present on the superconductor side of the m/s junction, however, the current distribution and power dissipation will depend on the *exact* distribution of these nonsuperconducting phases. Yet, if the minority nonsuperconducting phases are distributed *uniformly* on the surface of the inhomogeneous superconductive material, the effect of junction geometry and contact resistance on current distribution and power dissipation at the m/s junction and in the metal phase will be similar to those for pure superconducting materials. Nevertheless, the local power dissipation at or near the junction should in addition include the power dissipation in the nonsuperconducting phases at the superconductor side of the m/s junction.

VI. CONCLUSIONS

The primary current distribution and power dissipation are highly nonuniform in the system and are uniquely determined by the geometry of the metal-superconductor junctions. As the ratio of a/b increases, the primary current distribution becomes more uniform provided that dimension L is so long that it has no effect on distribution.

The secondary current distribution and power dissipation are further determined by the contact resistance of the m/s junction and the conductivity of the bulk metal phase in addition to the junction geometry. As the contact resistance of the interface or the conductivity of the metal phase increases, the secondary current distribution and power dissipation become more uniform for a given geometry, although the total power dissipation in the system slightly increases.

A finite contact resistance is necessary to ensure that the local current densities are below the critical current density of the superconducting phases and the current distribution and power dissipation are sufficiently uniform so that the performance of the device is stable and reliable.

A nonuniform contact resistance layer of suitable profile can redistribute the current more uniformly and hence reduce the total power dissipation in the system for a required j_{max}/j_{avg} ratio obtained by a uniform resistance of the contact layer.

ACKNOWLEDGMENT

This work was supported by the Division of Materials Science, Office of Basic Energy Service, United States Department of Energy, under contract No. DE-AC03-76SF00098 with the Lawrence Berkeley Laboratory.

NOTATIONS

a	height of the metal phase (cm)
b	length of the metal-superconductor junction (cm)
e^*	charge of electron pairs
$\mathbf{f}_n$	potential gradient at the m/s junction (V/cm)
$\mathbf{f}_0$	potential gradient at the end of the metal phase (Γ_2) (V/cm)
$\mathbf{j}$	current density in the metal phase (A/cm^2)
j_{avg}	average current density normal to the m/s junction (A/cm^2)
j_{cri}	critical current density of the superconducting phase (A/cm^2)
j_{max}	maximum current density normal to the m/s junction (A/cm^2)
j_n	current density normal to the m/s junction (A/cm^2)
J	total current normal to the m/s junction (A/cm^2)
L	length of the metal phase (cm)
m	number of the nodal points at the m/s junction
m^*	mass of electron pairs
n_s^*	number density of electron pairs
$\mathbf{n}$	unit vector normal to the m/s junction
$\mathbf{P}_n$	diagonal matrix containing boundary integration along the m/s junction
$\mathbf{P}_0$	diagonal matrix containing boundary integration along Γ_2
Q_b	Joule heat generated in the bulk metal phase (Joule)
Q_i	Joule heat generated at the m/s junction (Joule)
Q	total Joule heat generated in the system, $Q = Q_i + Q_b$
R	normalized interfacial resistance ($R = \alpha\sigma/b$), dimensionless
R_{eff}	effective total resistance of the system (ohm)
$\mathbf{U}_2$	unknown potentials within the domain (V)
ΔV_i	potential drop across the metal-superconductor interface (V)
α	specific interfacial resistance for linear contact (ohm-cm^2)
Φ_1	potential of the superconductor phase (V)
ϕ_j	nodal potential values (V)
Φ_0	potential at the end of the metal phase (V)
$\Phi(x, y)$	potential within the bulk metal phase (V)
Γ_1	insulated boundaries
Γ_2	end of the metal phase
Γ_3	surface of the metal phase adjacent to the m/s junction
Γ_e	boundary of an element
λ_L	London penetration depth
μ_0	permeability of free space
σ	conductivity of the bulk metal phase (ohm^{-1} cm^{-1})
Ω_e	domain of an element
Ω_m	domain of the bulk metal phase
$\Psi(\xi, \eta)$	approximation function in natural coordinates ξ, η

REFERENCES

[1]H. F. Moulton, *Proc. of the London Mathematical Society,* Ser. 2, **3**, 104 (1905).
[2]C. W. Tobias, "Numerical Evaluation of Current Distribution in Electrode Systems" (Abs. No. 323) in C.I.T.C.E. (International Committee for Electrochemical Thermodynamics and Kinetics) 13th meeting, Rome, September 24–29, 1962.
[3]R. N. Fleck, "Numerical Evaluation of Current Distribution in Electrochemical Systems" (M.S. Thesis), University of California, Berkeley, CA, September 1964 (URCL-11612).
[4]J. S. Newman, *Electrochemical Systems* (Prentice-Hall, Englewood Cliffs, NJ, 1972).
[5]C. W. Tobias and R. Wijsman, J. Electrochem. Soc. **100**, 459 (1953).
[6]J. S. Newman, J,. Electrochem. Soc. **113**, 1235 (1966).
[7]T. Richardson and L. C. De Jonghe, "Aluminum Cladding of High T_c Superconductor by Thermocompression Bonding", LBL #25499, July 1988.
[8]J. W. Ekin, T. M. Larson, N. F. Bergren, A. J. Nelson, A. B. Swartziander, L. L. Kazmerski, A. J. Panson, and B. A. Blankenship, Appl. Phys. Lett. **52**, 1819 (1988).
[9]Y. Tzeng, J. Electrochem. Soc. **135**, 1309 (1988).
[10]T. Van Duzer and C. W. Turner, *Principles of Superconductive Devices and Circuits* (Elsevier, New York, 1981).
[11]J. R. Schrieffer, *Theory of Superconductivity* (W. A. Benjamin, New York, 1964).